Phase transitions in wolframite-type $CdWO_4$ at high pressure studied by Raman spectroscopy and density-functional theory

R. Lacomba-Perales,[1] D. Errandonea,[2,*] D. Martinez-Garcia,[1] P. Rodríguez-Hernández,[3] S. Radescu,[3] A. Mujica,[3] A. Muñoz,[3] J. C. Chervin,[4] and A. Polian[4]

[1]*Departamento de Física Aplicada—ICMUV, MALTA Consolider Team, Universitat de València, Edificio de Investigación, c/Dr. Moliner 50, 46100 Burjassot, Valencia, Spain*

[2]*Departamento de Física Aplicada—ICMUV, MALTA Consolider Team, Fundación General de la Universitat de València, Edificio de Investigación, c/Dr. Moliner 50, 46100 Burjassot, Valencia, Spain*

[3]*Departamento de Física Fundamental II, MALTA Consolider Team, and Instituto de Materiales y Nanotecnología, Universidad de La Laguna, La Laguna 38205, Tenerife, Spain*

[4]*Institut de Minéralogie et de Physique des Milieux Condensés (IMPMC), CNRS UMR 7590, Université Pierre et Marie Curie, Paris 6 et 7, 140 rue de Lourmel, F-75015 Paris. France*

(Received 16 January 2009; revised manuscript received 12 February 2009; published 11 March 2009)

Room-temperature Raman scattering was measured in $CdWO_4$ up to 43 GPa. We report the pressure dependence of all the Raman-active phonons of the low-pressure wolframite phase. As pressure increases changes in the Raman spectra are detected at 20 and 35 GPa due to the onset of reversible structural phase transitions. We also report *ab initio* total-energy and lattice-dynamics calculations for the different phases of $CdWO_4$. They helped us determine the crystalline structure of the high-pressure phases. Experimental and theoretical results suggest the coexistence of two structures from 20 to 35 GPa: one with tetragonal symmetry and another with triclinic symmetry. Beyond 35 GPa the monoclinic β fergusonite is proposed as the structure of $CdWO_4$. The pressure evolution of the lattice parameters and the atomic positions of wolframite $CdWO_4$ are also theoretically calculated and an equation of state is reported.

DOI: 10.1103/PhysRevB.79.094105 PACS number(s): 62.50.−p, 63.20.dd, 64.70.K−, 63.20.dk

I. INTRODUCTION

Metal tungstates represent a very relevant class of inorganic compounds with many practical applications including phosphors, laser crystals, catalysis, and scintillation detectors.[1–4] In particular, cadmium tungstate ($CdWO_4$) is a wide-gap semiconductor with a band-gap energy close to 4 eV.[5,6] Tunsgtates of large divalent cations (Ca, Ba, Pb, Sr, and Eu) crystallize in the tetragonal scheelite structure [space group (SG): $I4_1/a$, $Z=4$] and those compounds of small divalent cations (Cd, Zn, Mg, and Fe) can take the wolframite structure (SG: $P2/c$, $Z=2$).[7] In wolframite-type $CdWO_4$, both Cd and W cations have octahedral oxygen coordination and each octahedron shares two corners with its neighbors. The WO_6 octahedra are distorted, with two of the W-O distances being shorter than the other four.

The behavior of AWO_4 compounds under pressure has been recently reviewed.[8] More specifically, scheelite-structured compounds have been studied using x-ray diffraction,[9–11] Raman spectroscopy,[12,13] and *ab initio* calculations;[14,15] the mechanisms involved in these transitions have been discussed;[16,17] and also a rule for the high-pressure structural sequence has been proposed.[8,18] In contrast with the scheelites, much less information is available about the pressure effects on the crystal structure of wolframites. Indeed, only two compounds of this subfamily have been studied so far. $ZnWO_4$ was recently studied up to 60 GPa by Raman spectroscopy and *ab initio* calculations.[19,20] A phase transition to a monoclinic β-fergusonite structure was found around 31 GPa and a second one to an orthorhombic structure was proposed to take place near 58 GPa.[19] Moreover the appearance of defects on single crystals of $ZnWO_4$ was detected under nonhydrostatic conditions near 12 GPa. These defects apparently were not present when argon was the pressure medium used in the experiments. $CdWO_4$ was previously studied by Raman spectroscopy under nonhydrostatic conditions up to 39 GPa.[21] In these experiments the appearance of defects was observed around 10 GPa and was attributed to the occurrence of a "subtle" phase transition.[21] However, this interpretation has been challenged in Ref. 19 and it is in contradiction with the 18 GPa transition pressure empirically estimated from the atomic radii of Cd, W, and O.[22] Indeed, a second phase transition was observed near 20 GPa.[21] The structure of the high-pressure phase of $CdWO_4$ has not been determined yet. Therefore, there are many issues to be clarified on the pressure effects on the crystalline structure of $CdWO_4$.

In this paper, in order to improve the knowledge of the physical properties of wolframite-type tungstates, as part of our project to study the structural stability of orthotungstates, we have carried out Raman spectroscopy measurements on $CdWO_4$ up to 43 GPa using neon as pressure-transmitting medium. The obtained results are interpreted on the basis of first-principles total-energy and lattice-dynamics calculations. Finally, experiments on $ZnWO_4$ were also performed up to 43 GPa to compare them with those performed using different pressure media.[19] The technical details of the experiments and calculations are described in Secs. II and III. The results are presented and discussed in Sec. IV. Finally, we present our conclusions in Sec. V.

II. EXPERIMENT DETAILS

The samples used in the present experiments were cleaved from a high-purity $CdWO_4$ single crystal provided by MTI corporation. The original crystal was oriented and polished along ⟨001⟩. The experiments on $ZnWO_4$ were performed on the same single crystal as that used in Ref. 19. It was confirmed by x-ray diffraction that $CdWO_4$ and $ZnWO_4$ have only one phase with the wolframite structure. Around 10-μm-thick plates of both samples were loaded simultaneously in a membrane diamond-anvil cell (DAC) (Ref. 23) together with ruby spheres of about 5 μm in diameter.[24] The surface of each plate was about 20×20 μm^2. The neon pressure-transmitting medium was loaded at 160 MPa.[25] The pressure was determined by the ruby fluorescence technique.[26] Room-temperature Raman experiments were performed in the backscattering geometry using the 514.5 nm (2.41 eV) line of an Ar^+-ion laser with a power of less than 100 mW before the DAC to avoid sample heating. Laser heating of the sample is negligible in the whole studied pressure range because the laser energy is always below the band gap of $CdWO_4$ and $ZnWO_4$ in the low-pressure and high-pressure phases: the band gap of both crystals is $Eg > 4$ eV,[5,6] with a positive pressure coefficient ($dEg/dP = 10$ meV/GPa),[27] and Eg is not expected to close by more than 1 eV at the pressure-induced phase transition.[28] A Mitutoyo 20X long working distance objective was employed for focusing the laser on the sample and for collecting the Raman spectra. The scattered light was analyzed with a Jobin-Yvon T64000 triple spectrometer equipped with a confocal microscope in combination with a liquid-nitrogen-cooled multichannel charge coupled device (CCD) detector. The spectral resolution was better than 1 cm^{-1}.

III. CALCULATION TECHNIQUE

Total-energy calculations and lattice-dynamics calculations were done within the framework of the density-functional theory (DFT) and the pseudopotential method using the Vienna *ab initio* simulation package (VASP) of which a detailed account can be found in Ref. 29. The exchange and correlation energy was taken in the generalized gradient approximation (GGA) according to Perdew-Burke-Ernzerhof (PBE) prescription.[30] The projector augmented wave (PAW) scheme[31] was adopted and the semicore $5p$ electrons of W were dealt with explicitly in the calculations. The set of plane waves used extended up to a kinetic-energy cutoff of 500 eV. This large cutoff was required to deal with the O atoms within the PAW scheme to ensure highly converged results. The Monkhorst-Pack grid used for Brillouin-zone integrations ensured highly converged results (to about 1 meV/f.u.). At each selected volume, the structures were fully relaxed to their equilibrium configuration through the calculation of the forces on atoms and the stress tensor; see Ref. 10. In the relaxed equilibrium configuration, the forces are less than 0.002 eV/Å and the deviation of the stress tensor from a diagonal hydrostatic form is less than 0.1 GPa. The highly converged results on forces are required for the calculation of the dynamical matrix using the direct force constant approach (or supercell method).[32] The construction of the dynamical matrix at the Γ point is particularly simple and involves separate calculations of the forces in which a fixed displacement from the equilibrium configuration of the atoms within the primitive unit cell is considered. Symmetry helps by reducing the number of such independent distortions and by reducing the amount of computational effort in the study of the analyzed structures considered in our work. Diagonalization of the dynamical matrix provides both the frequencies of the normal modes and their polarization vectors. It allows us to identify the irreducible representation and the character of the phonon modes at the zone center.

IV. RESULTS AND DISCUSSION

A. Raman measurements

Raman measurements on $CdWO_4$ were performed up to 43 GPa. A group theoretical analysis of the wolframite structure yields 36 lattice modes at the Γ point: $8\ A_g+10\ B_g+8\ A_u+10\ B_u$. The 18 even ($g$) vibrations are Raman-active modes and the 18 uneven (u) vibrations are infrared (IR) active. Symmetry assignments of the modes in the wolframite structure of $CdWO_4$ can be made based on previous experiments[21,33] and our *ab initio* calculations. Table I summarizes the phonon frequencies measured at the ambient pressure and the mode assignment. The reported frequencies are in very good agreement with those reported by Daturi *et al.*[33] and by Jayaraman *et al.*[21] In wolframite-type AWO_4 compounds, it has been proved that, as a first approximation, one can distinguish two types of vibrational modes: internal and external modes with respect to the WO_6 octahedra.[19] The internal modes correspond to normal vibrations of the WO_6 octahedra, while the external modes involve motions of WO_6 octahedra against the A atom (e.g., Cd or Zn). It is expected that the frequencies of the internal stretching modes will be higher than those of the external modes because the internal covalent bonding within the WO_6 octahedra is stronger than the external lattice binding. According to our calculations the internal stretching modes are the A_g modes located at 896, 706, 547, and 387 cm^{-1} and the B_g modes located at 771 and 687 cm^{-1}. This assignment can be tested by applying the Hardcastle and Wachs[34] approach that relates the frequencies of the internal modes of the WO_6 octahedra and the Pauling bond stretching in valence units.[19] Within this framework the estimated total valence is 5.895 in good agreement with the formal total valence of W (i.e., 6), which supports the assignment of the internal stretching modes we are proposing here.

Figure 1 shows the Raman spectra of $CdWO_4$ up to 43 GPa at selected pressures indicated in the figure. There are clearly three pressure ranges that will be discussed successively. Up to 20 GPa we have been able to follow the 18 Raman modes of wolframite. As it can be seen in Fig. 2, we did not observe any substantial change in the pressure dependence of the phonons up to this pressure. It is worth commenting here that we did not observe the domain formation reported at 10 GPa.[21] The fact that our experiments were done under nearly hydrostatic conditions at this pressure (neon pressure medium) gives support to the idea that the domain formation in $CdWO_4$ is related to poorly hydrostatic conditions (e.g., 4:1 methanol-ethanol pressure medium). We observed an analogous phenomenon in the measurements we performed in wolframite $ZnWO_4$. Apparently, the nonhydrostatic environment created by methanol-ethanol around

TABLE I. *Ab initio* and experimental phonon frequencies at 1 bar, pressure coefficients, and Grüneisen parameters of the Raman modes for the wolframite structure of $CdWO_4$. The asterisks indicate the internal stretching modes. The Grüneisen parameter has been calculated using the calculated bulk modulus $B_0 = 120$ GPa.

	Theory		Experiment			
Mode	ω [a] $[\mathrm{cm}^{-1}]$	$d\omega/dP$ [a] $[\mathrm{cm}^{-1}/\mathrm{GPa}]$	ω [a] $[\mathrm{cm}^{-1}]$	$d\omega/dP$ [a] $[\mathrm{cm}^{-1}/\mathrm{GPa}]$	γ [a]	ω [b] $[\mathrm{cm}^{-1}]$
B_g	67.4	0.89	78	0.52	0.80	77
A_g	97.4	0.36	100	0.69	0.83	99
B_g	110.8	0.91	118	1.02	1.04	117
B_g	125.9	0.74	134	0.82	0.73	133
B_g	141.7	1.03	148	1.51	1.22	148
A_g	177.0	0.70	177	0.71	0.48	177
A_g	220.2	0.11	229	0.29	0.15	229
B_g	238.5	1.86	249	2.14	1.03	248
B_g	252.1	1.70	269	1.41	0.63	269
A_g	286.9	0.12	306	0.04	0.02	307
B_g	337.9	4.14	352	4.55	1.55	351
A_g^*	356.9	2.39	388	2.33	0.72	387
B_g	490.1	2.63	514	3.86	0.90	514
A_g^*	530.5	1.51	546	2.32	0.51	547
B_g^*	655.5	3.68	688	4.35	0.74	687
A_g^*	683.6	3.32	707	3.92	0.67	706
B_g^*	742.5	3.95	771	4.30	0.67	771
A_g^*	864.4	2.88	897	3.66	0.49	896

[a]This work.
[b]Reference 33.

10–12 GPa (Ref. 35) induces multiple twining in monoclinic wolframite. The domains optically observed are possibly a consequence of it. Figure 2 shows the pressure evolution of different Raman modes of $CdWO_4$. From Fig. 2 we extracted the pressure dependence of the Raman modes of wolframite up to 20 GPa. Most of the modes have a slightly nonlinear behavior. In addition, the A_g modes with frequencies of 229 and 306 cm^{-1} at ambient pressure are basically not affected by pressure. The same fact was observed by Jayaraman *et al.*[21] and also for the equivalent modes of $ZnWO_4$.[19] Another interesting fact to remark is that some modes collapse near 20 GPa, close to 700 cm^{-1} and around 500–550 cm^{-1}, for example. This is suggesting a tendency to a gradual symmetry increase in wolframite.

Table I also summarizes the pressure coefficients ($\partial\omega/\partial P$) of the Raman modes of wolframite $CdWO_4$ at zero pressure and their Grüneisen parameters ($\gamma = B_0/\omega \cdot \partial\omega/\partial P$, where B_0 is the bulk modulus). The mode Grüneisen parameters have been calculated using $B_0 = 120$ GPa obtained from our *ab initio* calculations. This value is in good agreement with the value extracted from x-ray diffraction experiments performed up to 8.2 GPa (Ref. 36) and with that estimated from the cation formal charge of Cd and the mean Cd-O distance using the empirical law reported in Ref. 10. Note (Table I) that with the exception of the two pressure insensitive Ag modes, the internal stretching modes of the WO_6 octahedra are among those with the smaller Grüneisen parameters. The same fact was reported for $ZnWO_4$ (Ref. 19) and is related with the incompressibility of the WO_6 octahedra.[36]

Beyond 20 GPa, important changes take place in the Raman spectra (see Fig. 1). The peak number changes from 18 to 27 (see Fig. 2). Additional changes are observed around 35 GPa. Beyond this pressure there are again 18 Raman modes but at different frequencies than those observed in the low-pressure phase. It is important to note that at 35 GPa also a drastic color change occurs in $CdWO_4$, with it becoming yellow. Apparently two phase transitions take place in $CdWO_4$ upon compression: the first one around 20 GPa (to a phase we will denote as phase II) and the second one around 35 GPa (to phase III). Upon pressure release, the changes in the Raman spectra are reversible. However we observed some hysteresis; $CdWO_4$ goes back from III to II at 26.3 GPa and from II to I at 16.4 GPa. The first transition is in excellent agreement with the results reported in Ref. 21. However, in this work the second transition was not detected although the experiments were performed up to 38 GPa. Moreover, the high-pressure Raman spectra present very broad and weak peaks that may be due to the use of the ethanol-methanol mixture as a pressure-transmitting medium, which makes their identification difficult. In addition, in our experiments, up to 38 GPa we observed the coexistence of peaks corresponding to phase II and phase III. Differences between the Raman spectra of phases II and III can be only clearly seen beyond 38 GPa. These two facts could have precluded the detection of the second transition in Ref. 21.

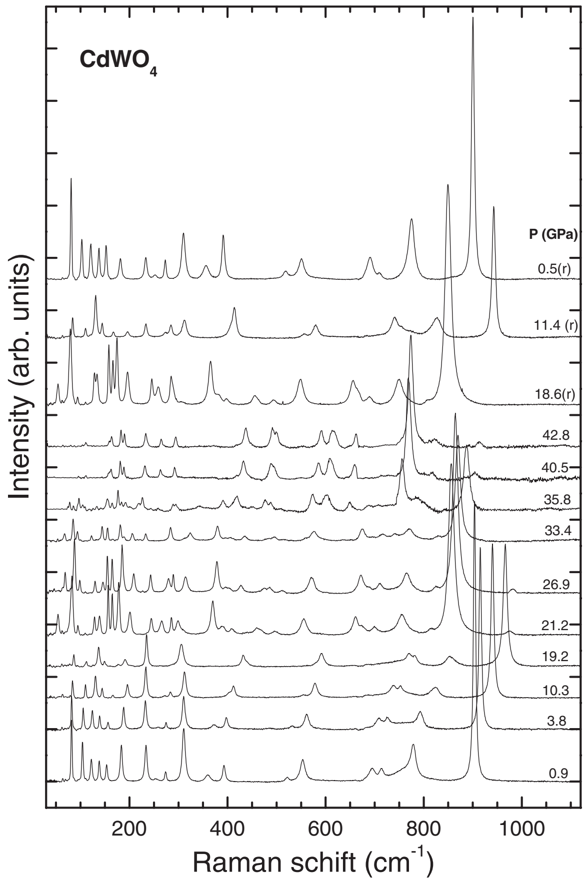

FIG. 1. Raman spectra of $CdWO_4$ at different pressures. All the spectra were measured on pressure increase with the exception of those marked with (*r*), which were taken on pressure release.

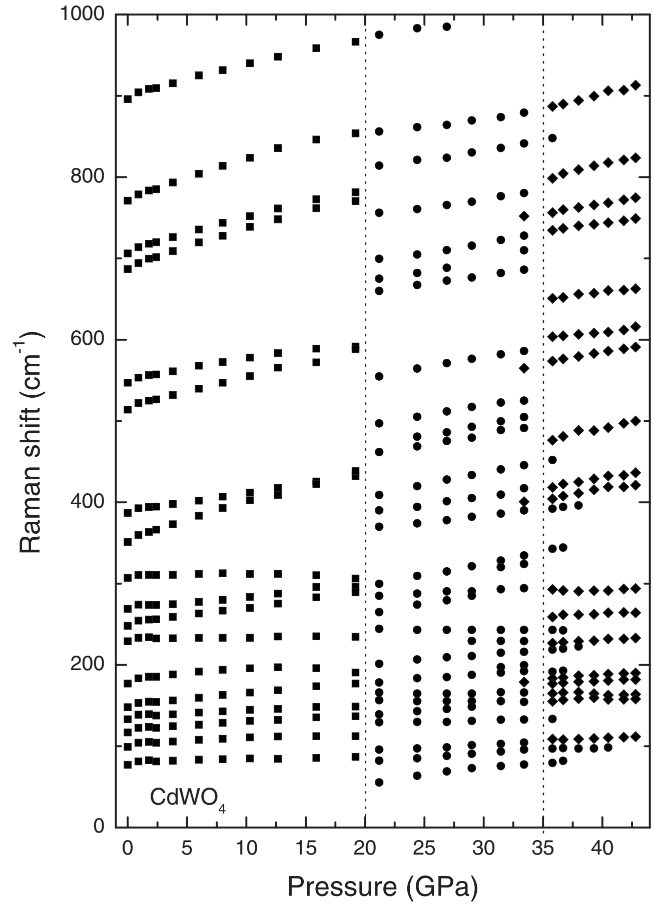

FIG. 2. Pressure dependence of the Raman mode frequencies of wolframite (squares), phase II (circles), and phase III (diamonds) in $CdWO_4$.

The pressure dependence of the phonons for phases II and III can be seen in Fig. 2. Table II presents the phonon frequencies and their pressure dependences for phase II. The frequencies are in good agreement with those reported in Ref. 21. Table III gives the same information but for phase III. A remarkable feature is that the highest frequency mode drops at the II–III transition by nearly 200 cm^{-1}. As we discussed above this mode is related to internal vibrations of the W-O polyhedra. Thus, this fact suggests that a W-O coordination increase takes place at the phase transition. When the W coordination increases, the W-O bond lengths usually do it too for steric reason. The result is a drop in the frequency of the internal stretching modes. This behavior was observed in other AWO_4 tungstates,[12,19] in particular in $ZnWO_4$ at the wolframite-β-fergusonite transition. Indeed, we believe it is not a mere coincidence: the resemblance of the Raman spectra of phase III for $CdWO_4$ with those of the β-fergusonite structure of $ZnWO_4$. These facts will be considered for identifying the structure of the high-pressure phases of $CdWO_4$ with the help of *ab initio* calculations.

To conclude this section we would like to briefly comment on the experiments in $ZnWO_4$. These experiments confirm previous results obtained using argon as pressure medium.[19] The onset of the pressure-induced phase transition is found at 30 GPa, but the low-pressure phase and the high-pressure phase coexist up to 36 GPa. The high-pressure phase remains stable up to 43 GPa. In addition, as we comment above, no domain formation is observed, in contrast with the findings of experiments done using a 16:3:1 methanol-ethanol-water as pressure medium.[19] The Raman spectra of the high-pressure phase and the pressure dependence of the phonons are consistent with the β-fergusonite structure previously proposed for it.[19]

B. *Ab initio* calculations

To help with the interpretation of our experimental results, *ab initio* total-energy and lattice-dynamics calculations were performed for $CdWO_4$. Along with the wolframite structure, we have considered other structures on account of their observation or postulation in previous high-pressure works for related compounds: triclinic $CuWO_4$-type (SG: $P\bar{1}$), orthorhombic disordered wolframite (SG: *Pbcn*), monoclinic *M* fergusonite (SG: $I2/a$), monoclinic M' fergusonite (SG: $P2_1/c$), monoclinic β fergusonite (SG: $C2/c$), tetragonal scheelite (SG: $I4_1/a$), monoclinic $HgWO_4$-type (SG: $C2/c$), monoclinic $BaWO_4$-II-type (SG: $P2_1/n$), orthorhombic *Cmca*, and monoclinic α-$MnMoO_4$ (SG: $C2/m$). Figure 3 shows the energy vs volume curves for the most competitive structures. The common tangent construction enables to deduce the transition pressure and the equilibrium pressure.[37]

TABLE II. Frequencies around 27 GPa and pressure coefficients of the Raman modes of the phase II of $CdWO_4$. The frequencies and pressure coefficients obtained after *ab initio* calculations are also given.

Theory						Experiment		
	Scheelite-type			$CuWO_4$ -type				
Mode	ω [a] $[cm^{-1}]$ 27.8 GPa	$d\omega/dP$ [a] $[cm^{-1}/GPa]$	Mode	ω [a] $[cm^{-1}]$ 26.8 GPa	$d\omega/dP$ [a] $[cm^{-1}/GPa]$	ω [a] $[cm^{-1}]$ 26.9 GPa	$d\omega/dP$ [a] $[cm^{-1}/GPa]$	ω [b] $[cm^{-1}]$ 28 GPa
B_g	77.2	1.39				69	1.96	
			A_g	88.8	1.86	88	1.94	84
			A_g	106.1	0.16	99	0.09	111
E_g	124.2	0.79				130	0.38	
			A_g	133.9	0.94			
			A_g	144.5	1.21	146	1.35	150
			A_g	171.4	0.64	155	0.97	
E_g	174.5	1.40						
			A_g	176.9	−0.20	165	0.19	
B_g	188.7	1.42				185	1.26	182
			A_g	222.6	0.94	209	1.26	211
A_g	255.8	0.19				243	−0.06	240
			A_g	292.3	2.04	279	2.53	280
			A_g	294.6	1.57	290	0.99	
			A_g	308.4	4.56	315	3.00	311
A_g	348.1	1.59				378	1.65	375
B_g	348.1	1.80						
E_g	393.7	3.05				401	2.31	
			A_g	422.0	2.59	428	3.03	432
			A_g	448.8	3.96			462
B_g	479.8	3.16				475	2.51	
E_g	480.1	3.16				486	2.72	
			A_g	564.0	1.79	512	2.33	
			A_g	572.9	2.32	571	2.62	562
						673	−0.82	
						688	2.81	
			A_g	757.7	2.10	710	1.60	716
			A_g	774.7	2.11	766	2.12	761
E_g	805.0	1.57						
B_g	844.6	1.33						
			A_g	852.2	2.89	824	2.23	
A_g	885.56	1.54				864	2.04	877
			A_g	944.7	1.91	975	1.83	985

[a]Present work.
[b]Reference 21.

In the figure we only reported those structures that play a relevant role in the high-pressure structural behavior of $CdWO_4$. According to the calculations wolframite is the most stable structure from ambient pressure up to 21.2 GPa. Beyond this pressure other structures become energetically more favorable, which is in good agreement with the phase transition detected in the Raman experiments at 20 GPa. For the wolframite structure at ambient pressure, the calculations gave $a=5.096$ Å, $b=6.015$ Å, $c=5.136$ Å, and $\beta=91.17°$. The obtained atomic positions are summarized in Table IV. The calculated unit-cell parameters are slightly larger than the experimental values ($a=5.028$ Å, $b=5.862$ Å, $c=5.067$ Å, and $\beta=91.5°$).[36] This small overestimation is within the typical reported systematic errors in DFT-GGA calculations. The calculated equation of state (EOS) of wolframite $CdWO_4$ is given by the following parameters $V_0=157.4$ Å,[3] $B_0=120$ GPa, and $B_0'=3.5$ (the zero pressure volume, the bulk modulus, and its pressure derivative, respectively). They were obtained from our calculations using a third-order Birch-Murnagahn EOS.[38] The calculated EOS

TABLE III. Frequencies around 38 GPa and pressure coefficients of the Raman modes of the phase III of $CdWO_4$. The frequencies and pressure coefficients obtained after *ab initio* calculations are also given.

Mode	Theory ω [cm^{-1}] 38.4 GPa	Theory $d\omega/dP$ [cm^{-1}/GPa]	Experiment ω [cm^{-1}] 38 GPa	Experiment $d\omega/dP$ [cm^{-1}/GPa]
A_g	113.0	1.26	109	0.65
B_g	156.0	0.35	158	0.19
B_g	156.1	0.36	167	−0.20
B_g	204.6	0.88	179	0.64
B_g	204.8	0.97	187	0.91
A_g	248.3	0.53	229	0.73
B_g	293.3	0.95	262	0.48
B_g	293.4	0.96	291	0.49
A_g	369.9	3.10	411	2.28
A_g	523.9	2.60	425	2.26
B_g	588.4	2.82	488	3.11
B_g	588.6	2.97	579	2.48
A_g	680.1	3.06	607	2.04
A_g	693.1	1.36	656	1.63
B_g	737.4	1.30	742	1.96
B_g	737.5	1.44	763	2.20
A_g	769.2	1.37	809	3.08
A_g	795.7	3.52	894	3.70

parameters agree well with those extracted from low-pressure x-ray diffraction data.[36] The inset of Fig. 3 shows the calculated *P-V* relationship which corresponds to the reported EOS.

Figure 4 shows the pressure dependence obtained from our calculations for the lattice parameters and the monoclinic β angle of wolframite $CdWO_4$. There it can be seen that as in other orthotungstates the compressibility is highly anisotropic, with the *b* axis being the most compressible. As a consequence the b/a axial ratio decreases by about 6% from ambient pressure to the transition pressure. In contrast the c/a axial ratio decreases only by 0.5%. At the same time, compression also causes an increase in the β angle. A similar increase was experimentally observed in Ref. 36. On the other hand, the changes in the atomic positions with pressure are insignificant for Cd and W but are not negligible for O (see Table IV). The anisotropic compressibility of wolframite $CdWO_4$ can be understood in terms of hard anionlike WO_6 octahedra surrounded by charge compensating Cd cations. Figure 5 shows the calculated pressure dependence for the Cd-O and W-O interatomic distances. As it can be seen, the Cd-O bond length decreases faster with pressure than the W-O bond length. In particular, the largest Cd-O bonds are the most compressible, which cause a gradual reduction in the anisotropy of the CdO_6 octahedra upon compression. A similar incompressibility of the W-O bonds has been observed in $ZnWO_4$.[19] This means that when pressure is applied the WO_6 units remain essentially undistorted and the reduction in the unit-cell size is mainly associated with the compression of the Cd-O octahedral environment. As in $ZnWO_4$, in $CdWO_4$ along the *b* axis the WO_6 units are directly aligned, whereas along the *a* and *c* axes there is a Cd cation between two WO_6 octahedra. Thus, the different arrangement of hard WO_6 octahedra along the different axes accounts for their different compressibility.

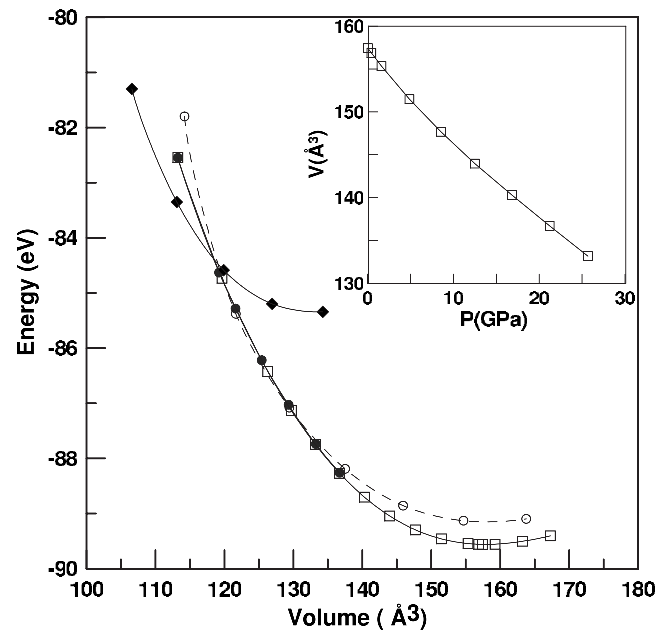

FIG. 3. Energy-volume curves calculated for $CdWO_4$. Squares (wolframite), solid circles ($CuWO_4$-type), empty circle (scheelite), and diamonds (β fergusonite). The inset shows the calculated pressure dependence of the volume (symbols) and the obtained equation of state (line) for the wolframite phase.

In addition to the structural calculations we have also performed lattice-dynamical calculations for wolframite $CdWO_4$. Table I compares the calculated frequencies and pressure coefficients for the Raman modes with the experi-

TABLE IV. Calculated atomic positions for Cd, W, and O atoms in wolframite $CdWO_4$ at different pressures.

Wolframite at 1 bar; a=5.096 Å, b=6.015 Å, c=5.136 Å, β=91.17°	
Cd (site: 2*f*)	x=0.5, y=0.6919, z=0.25
W (site: 2*e*)	x=0, y=0.1758, z=0.25
O_1 (site: 4*g*)	x=0.2419, y=0.3663, z=0.3839
O_2 (site: 4*g*)	x=0.1999, y=0.9037, z=0.4481
Wolframite at 21.2 GPa; a=4.961 Å, b=5.536 Å, c=4.984 Å, β=93.04°	
Cd (site: 2*f*)	x=0.5, y=0.7123, z=0.25
W (site: 2*e*)	x=0, y=0.1911, z=0.25
O_1 (site: 4*g*)	x=0.2421, y=0.3982, z=0.3953
O_2 (site: 4*g*)	x=0.2133, y=0.9141, z=0.4677

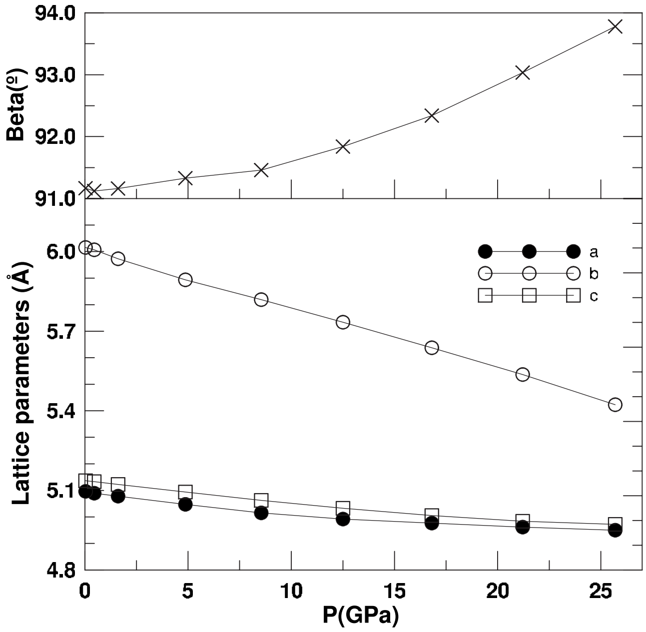

FIG. 4. Theoretically calculated pressure dependence of the lattice parameters and the monoclinic β angle of the wolframite structure of $CdWO_4$.

mental ones. The agreement between calculations and experiments for the low-pressure phase is reasonably good and similar to that obtained in $ZnWO_4$ and other orthotungstates.[12,19] This fact gives credibility to the lattice-dynamics calculations performed for the high-pressure phases of $CdWO_4$. As we discussed above, the calculated eigenmodes for wolframite $CdWO_4$ indicate that there are Raman modes that involve basically a movement of the WO_6 octahedra as rigid units and others that imply internal vibrations of these octahedra. Therefore, despite this, external and internal modes show similar Grüneisen parameters and this prevents a simple distinction between them. However, as in scheelite-structured compounds,[12] this distinction can still be applied to wolframite structured compounds as we did along the paper, and it has been done for $ZnWO_4$.[19] The isolation of the WO_6 octahedra is also evident from the incompressibility of the W-O bonds already described. The internal stretching modes are those indicated by asterisks in Table I. Note that the larger discrepancies between calculations and experiments are found for these particular modes. The same fact was also observed in scheelite-structured tungstates.[12] From our calculations we also obtained the frequencies of the infrared-active modes whose calculated frequencies and pressure coefficients are reported in Table V. As it happens with the calculated Raman frequencies, the agreement with the experiments[33] is better for the low-frequency modes than for the high-frequency modes. Unfortunately, there are no experimental data available to compare with the pressure behavior of the IR-active phonons. According to our calculations, the IR modes are less pressure sensitive than the Raman modes (see Tables I and V).

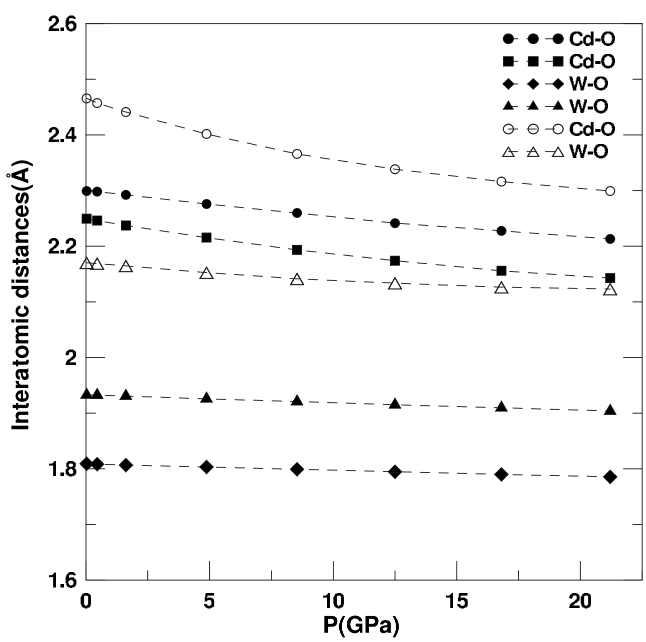

FIG. 5. Theoretically calculated pressure dependence of the Cd-O and W-O interatomic distances in the low-pressure phase of $CdWO_4$.

TABLE V. Mode frequencies, pressure coefficients, and Grüneisen parameters of the calculated IR modes in wolframite $CdWO_4$ at zero pressure.

Mode	Theory ω [a] $[cm^{-1}]$	Theory $d\omega/dP$ [a] $[cm^{-1}/GPa]$	Theory γ	Experiment ω [b] $[cm^{-1}]$
B_u	0			
B_u	0			
A_u	1.70			
B_u	105.6	−0.17	−0.19	107
A_u	121.5	0.10	0.10	131
B_u	145.0	0.07	0.06	161
B_u	225.9	0.15	0.08	230
B_u	252.9	0.06	0.03	
B_u	255.2	0.36	0.17	260
A_u	270.1	0.09	0.04	310
A_u	322.1	0.03	0.01	354
A_u	379.4	0.30	0.09	408
B_u	420.9	0.38	0.11	455
A_u	471.4	0.35	0.09	510
B_u	524.2	0.38	0.09	595
A_u	626.8	0.39	0.07	693
B_u	743.6	0.38	0.06	835
A_u	839.1	0.34	0.05	884

[a]Present work.
[b]Reference 33.

Let us concentrate now on the high-pressure phases of $CdWO_4$. In our experiments we found evidence of a phase transition at 20 GPa. Calculations found that at 21 GPa wolframite becomes unstable against two competing structures: tetragonal scheelite ($I4_1/a$) and triclinic $CuWO_4$-type ($P\bar{1}$)

TABLE VI. Structural parameters of scheelite (27.8 GPa) and $CuWO_4$-type (26.9 GPa) $CdWO_4$.

Scheelite (SG:$I4_1/a$,Z=4); $a=b=4.996$ Å, $c=10.370$ Å	
Cd (site: 4b)	$x=0$, $y=0.25$, $z=0.625$
W (site: 4a)	$x=0$, $y=0.25$, $z=0.125$
O (site: 16f)	$x=0.2378$, $y=0.9354$, $z=0.9708$
$CuWO_4$-type (SG: $P\bar{1}$, Z=2); $a=4.949$ Å, $b=5.396$ Å, $c=4.966$ Å, $\alpha=89.972°$, $\beta=94.001°$, $\gamma=89.975°$	
Cd (site:2i)	$x=0.4998$, $y=0.7241$, $z=0.2496$
W (site:2i)	$x=0.0003$, $y=0.1977$, $z=0.2500$
O_1 (site:2i)	$x=0.2412$, $y=0.4093$, $z=0.4014$
O_2 (site:2i)	$x=0.2181$, $y=0.9191$, $z=0.4781$
O_3 (site:2i)	$x=0.2405$, $y=0.5902$, $z=0.9013$
O_4 (site:2i)	$x=0.2183$, $y=0.0803$, $z=0.9781$

(see Fig. 3). It should be noted here that our calculations do not include the zero-point energy and temperature effects and that the energy differences (3–4 meV/atom) are in the range of the standard DFT errors. Therefore, the conclusions on the structure of phase II have been obtained from the combination of our total-energy and lattice-dynamics calculations with our experimental results. The structural parameters of the tetragonal and triclinic structures that compete with wolframite are summarized in Table VI for a pressure close to 27 GPa. At the Γ point, scheelite has 13 Raman-active modes: 3 A_g, 5 B_g, and 5 E_g and $CuWO_4$-type 18:18 A_g. In the experiments from 20 to 35 GPa we found at least 26–28 modes. Most of these modes, in particular those with a frequency larger than 240 cm^{-1}, do not coincide with the Raman frequencies expected for wolframite $CdWO_4$ and have different pressure coefficients than them (see Fig. 2). Furthermore, any other candidate structure taken into account in the calculations, in addition to scheelite and $CuWO_4$-type, has either too many or too few Raman modes and is not energetically competitive. Based on the results reported in Fig. 3 and the typical polytypism and phase coexistence of AWO_4 compounds at ambient and high pressure,[8,39] one possibility to explain the Raman results of phase II is the coexistence of the scheelite and $CuWO_4$-type structures. The coexistence of any of these structures with wolframite has been discarded because it does not provide a satisfactory explanation to the experimental results; however, it cannot be completely ruled out. Note that the $CuWO_4$-type structure has been observed to coexist with monoclinic or tetragonal structures in many related compounds such as $MgWO_4$.[40] Although this structure is triclinic, it is topologically related to wolframite. The main difference is that WO_6 and CdO_6 octahedra are more distorted. In addition, there is a group–subgroup relationship between the space groups $P\bar{1}$ and $P2/c$, which makes the wolframite-to-$CuWO_4$-type transition reasonable from the crystallochemical point of view. According to the calculations, the transition between both structures takes place without a volume change. This is consistent with the ferroelastic character of the same transition in $CuWO_4$-$ZnWO_4$ alloys.[41] On the other hand, scheelite is the structure of $CdMoO_4$ and it is a possible high-pressure phase of $CdWO_4$ according to the cation-size systematic developed by Bastide.[8] In addition, a crystallographic relationship also exists between scheelite and wolframite and it has been suggested that one can be the high-pressure structure of the other.[42] In the case of the wolframite-scheelite transition we found a volume change of about 2%, suggesting that this transformation is a first-order transition. Based on packing efficiency the scheelite structure is more favorable than the $CuWO_4$-type one. However, given the first-order nature of the wolframite-scheelite transition and the second-order nature of the wolframite-$CuWO_4$-type transition, the presence of kinetic barriers could favor the coexistence of the triclinic and tetragonal structures under compression. In summary, a two-phase mixture could be a plausible explanation for the experimental results obtained in phase II. To check this hypothesis we calculate the Raman-active phonons at different pressures for the scheelite and $CuWO_4$-type structures. They are compared with the experiments in Table II. The same kind of agreement, as for the wolframite phase, is obtained for the calculated modes in phase II. Only the two weak peaks around 680 cm^{-1} in the experiments cannot be satisfactory explained by the calculations (note that they cannot be assigned either to wolframite $CdWO_4$, which in the pressure range of interest does not have any Raman mode between 570 and 760 cm^{-1}; see Fig. 1 and Table I). Therefore, we concluded that the phase coexistence is a reasonable explanation for the experiments. High-pressure x-ray diffraction studies are needed to fully confirm it. However, the good predictions made by *ab initio* calculations in other AWO_4 compounds[10,14,19] and the fact that calculations explain 25 out of the 27 measured peaks and also the pressure dependence of most of the phonons give credibility to the proposed phase scheme.

TABLE VII. Structural parameters of β fergusonite (38.8 GPa) $CdWO_4$.

β fergusonite ($C2/c$,Z=4); $a=7.614$ Å, $b=7.802$ Å, $c=5.384$ Å, $\beta=134.998°$	
Cd (site:4e)	$x=0$, $y=0.3750$, $z=0.25$
W (site:4e)	$x=0$, $y=0.8750$, $z=0.25$
O_1 (site:8f)	$x=0.1347$, $y=0.5902$, $z=0.9549$
O_2 (site:8f)	$x=0.3396$, $y=0.3402$, $z=0.7756$

In agreement with our Raman measurements, *ab initio* calculations also predict a second phase transition near 35 GPa. This high-pressure phase (phase III) has a monoclinic β-fergusonite structure ($C2/c$). This structure implies an increase in the W-O coordination number from 4+2 to 4+4 and of the Cd-O coordination from 4+2 to 8. The structural parameters of β fergusonite are summarized in Table VII. It is important to note that this structure is also found to be the high-pressure structure in $ZnWO_4$ beyond 36 GPa,[19] but in this case the transition takes place directly from wolframite to β fergusonite. A comparison of our lattice-dynamics calculations with the Raman spectra collected in phase III of $CdWO_4$ provides additional support to the characterization of this phase as β fergusonite. This structure has 18 Raman-active modes at the Γ point: 8 A_g and 10 B_g, as observed experimentally. Table III compares the calculated phonons and their pressures dependences for β fergusonite with those determined from our experiments around 38 GPa. The agreement is similar to that obtained in the low-pressure phases. The largest differences are observed again for the high-frequency modes. Furthermore, it is interesting to point out that the experimental Raman spectra of phase III of $CdWO_4$ (see Fig. 1) resemble very much those of phase II of $ZnWO_4$ (β fergusonite) but shifted to higher frequencies (see Ref. 19). This also happens if we compare the wolframite phase of both compounds, and it is due to the larger atomic mass of the Cd cation. So the similitude of the Raman spectra of $CdWO_4$ III and $ZnWO_4$ II is in good agreement with the predictions of the calculations. X-ray diffraction experiments are needed to confirm that beyond 35 GPa the β-fergusonite phase becomes stable in $CdWO_4$, but the evidence we presented here points all toward this conclusion.

V. SUMMARY

We performed room-temperature Raman scattering measurements under pressure in $CdWO_4$ up to 43 GPa using neon as pressure medium. The frequency pressure dependence of all first-order modes of the wolframite phase has been measured up to the completion of a phase transition around 20 GPa. This value of the transition pressure is in good agreement with the estimated transition pressure according to our *ab initio* total-energy calculations. The *ab initio* calculations also allow us to determine the pressure evolution of the unit-cell parameters of wolframite $CdWO_4$ and to show that its compression is highly anisotropic. This behavior is related to the different compressibility of Cd-O and W-O bonds, the latter being much more rigid than the former. The calculated phonon frequencies (and pressure dependences) for wolframite agree reasonably well with the experiments. Calculations also help us to propose a characterization for phase II. They suggest that it consists in a mixture of a triclinic phase and a tetragonal phase normally observed in other tungstates. The calculated phonons for phase II reasonably agree with the experiments. A second pressure-induced phase transition is found at 35 GPa both in experiments and calculations. There is enough evidence to propose that phase III has a monoclinic β-fergusonite structure. Both phase transitions are reversible with some hysteresis. The stability pressure range of phase II is reduced on pressure release. Additional experiments were performed for $ZnWO_4$ using neon as pressure medium. The obtained results confirm those previously reported from experiments performed in argon and even less hydrostatic pressure media. According to our experiments and calculations the monoclinic β-fergusonite phase is stable at high pressure for the wolframites $ZnWO_4$ and $CdWO_4$, although in this last case the transition from wolframite to β fergusonite occurs through an intermediate phase. Finally, we would like to mention that up to 43 GPa we did not find any evidence suggesting that either $CdWO_4$ or $ZnWO_4$ amorphizes or decomposes. We also concluded that nonhydrostatic conditions can be the cause of the domain formation observed when working using methanol-ethanol (or similar media).[19,21] This phenomenon is not observed when working with neon medium or argon pressure-transmitting medium.

ACKNOWLEDGMENTS

This work was made possible through financial support of the MICINN of Spain under Grants No. MAT2007-65990-C03-01, MAT2007-65990-C03-03, and CSD2007-00045 and of the Generalitat Valenciana under Grant No. GV2008/112. R.L.-P. thanks the support from the MICINN through the "FPU" program.

*Corresponding author; daniel.errandonea@uv.es

[1] W. Chen, Y. Inagawa, T. Omatsu, M. Tateda, N. Takeuchi, and Y. Usuki, Opt. Commun. **194**, 401 (2001).

[2] P. Lecoq, I. Dafinei, E. Auffray, M. Scheegans, M. V. Korzhik, O. V. Missetvich, V. B. Pavlenko, A. A. Fedorov, A. N. Annenkov, V. L. Kostylev, and V. D. Ligun, Nucl. Instrum. Methods Phys. Res. A **365**, 291 (1995).

[3] M. Ishii and M. Kobayashi, Prog. Cryst. Growth Charact. Mater. **23**, 245 (1992).

[4] G. Fagherazzi and N. Pernicone, J. Catal. **16**, 321 (1970).

[5] R. Lacomba-Perales, J. Ruiz-Fuertes, D. Errandonea, D. Martınez-Garcıa, and A. Segura, EPL **83**, 37002 (2008).

[6] M. Fujita, M. Itoh, T. Katagiri, D. Iri, M. Kitaura, and V. B. Mikhailik, Phys. Rev. B **77**, 155118 (2008).

[7] A. W. Sleight, Acta Crystallogr., Sect. B: Struct. Crystallogr. Cryst. Chem. **B28**, 2899 (1972).

[8] D. Errandonea and F. J. Manjon, Prog. Mater. Sci. **53**, 711 (2008).

[9] V. Panchal, N. Garg, A. K. Chauhan, B. Sangeeta, and S. M. Sharma, Solid State Commun. **130**, 203 (2004).

[10] D. Errandonea, J. Pellicer-Porres, F. J. Manjon, A. Segura, Ch. Ferrer-Roca, R. S. Kumar, O. Tschauner, P. Rodriguez-Hernandez, J. Lopez-Solano, S. Radescu, A. Mujica, A. Muñoz, and G. Aquilanti, Phys. Rev. B **72**, 174106 (2005).

[11] D. Errandonea, Phys. Status Solidi B **242**, R125 (2005).

[12] F. J. Manjon, D. Errandonea, N. Garro, J. Pellicer-Porres, J. Lopez-Solano, P. Rodriguez-Hernandez, S. Radescu, A. Mujica, and A. Muñoz, Phys. Rev. B **74**, 144112 (2006), and references therein.

[13] D. Christofilos, K. Papagelis, S. Ves, G. A. Kourouklis, and C. Raptis, J. Phys.: Condens. Matter **14**, 12641 (2002).

[14] D. Errandonea, J. Pellicer-Porres, F. J. Manjon, A. Segura, Ch. Ferrer-Roca, R. S. Kumar, O. Tschauner, J. Lopez-Solano, P. Rodríguez-Hernandez, S. Radescu, A. Mujica, A. Muñoz, and G. Aquilanti, Phys. Rev. B **73**, 224103 (2006).

[15] J. López-Solano, P. Rodrıguez-Hernández, S. Radescu, A. Mujica, A. Muñoz, D. Errandonea, F. J. Manjón, J. Pellicer-Porres, N. Garro, A. Segura, Ch. Ferrer-Roca, R. S. Kumar, O.

Tschauner, and G. Aquilanti, Phys. Status Solidi B **244**, 325 (2007).
[16] D. Errandonea, EPL **77**, 56001 (2007).
[17] D. Errandonea and F. J. Manjon, Mater. Res. Bull. **44**, 807 (2009).
[18] F. J. Manjón and D. Errandonea, Phys. Status Solidi B **246**, 9 (2009).
[19] D. Errandonea, F. J. Manjon, N. Garro, P. Rodriguez-Hernandez, S. Radescu, A. Mujica, A. Muñoz, and C. Y. Tu, Phys. Rev. B **78**, 054116 (2008).
[20] A. Perakis, E. Serestepoulous, and C. Raptis, High Press. Res. **18**, 181 (2000).
[21] A. Jayaraman, S. Y. Wang, and S. K. Sharma, Curr. Sci. **69**, 44 (1995).
[22] D. Errandonea, F. J. Manjon, M. Somayazulu, and D. Häusermann, J. Solid State Chem. **177**, 1087 (2004).
[23] J. C. Chervin, B. Canny, J. M. Besson, and Ph. Pruzan, Rev. Sci. Instrum. **66**, 2595 (1995).
[24] J. C. Chervin, B. Canny, and M. Mancinelli, High Press. Res. **21**, 305 (2001).
[25] B. Couzinet, N. Dahan, G. Hamel, and J. C. Chervin, High Press. Res **23**, 409 (2003).
[26] H. K. Mao, P. M. Bell, J. W. Shaner, and D. J. Steinberg, J. Appl. Phys. **49**, 3276 (1978).
[27] R. Lacomba, M.S. thesis, Universitat de Valencia, 2007.
[28] D. Errandonea, D. Martinez-Garcia, R. Lacomba-Perales, J. Ruiz-Fuertes, and A. Segura, Appl. Phys. Lett. **89**, 091913 (2006).
[29] G. Kresse, computer code VASP. See: http://cms.mpi.univie.ac.at/vasp.
[30] J. P. Perdew, K. Burke, and M. Ernzerhof, Phys. Rev. Lett. **77**, 3865 (1996).
[31] P. E. Blöchl, Phys. Rev. B **50**, 17953 (1994); G. Kresse and D. Joubert, *ibid.* **59**, 1758 (1999).
[32] K. Parlinski, computer code PHONON. See: http://wolf.ifj.edu.pl/phonon.
[33] M. Daturi, G. Busca, M. M. Borel, A. Leclaire, and P. Piaggio, J. Phys. Chem. B **101**, 4358 (1997).
[34] F. D. Hardcastle and I. E. Wachs, J. Raman Spectrosc. **26**, 397 (1995).
[35] D. Errandonea, Y. Meng, M. Somayazulu, and D. Häusermann, Physica B **355**, 116 (2005).
[36] J. Macavei and H. Schulz, Z. Kristallogr. **207**, 193 (1993).
[37] A. Mujica, A. Rubio, A. Muñoz, and R. J. Needs, Rev. Mod. Phys. **75**, 863 (2003).
[38] F. Birch, J. Geophys. Res. **83**, 1257 (1978).
[39] R. Lacomba-Perales, D. Martínez-García, D. Errandonea, Y. Le Godec, J. Philippe, and G. Morard, High Press. Res. **29**, 109 (2009).
[40] V. B. Mikhailik, H. Kraus, V. Kapustyanyk, M. Panasyuk, Yu Prots, V. Tsybulskyi, and L. Vasylechko, J. Phys.: Condens. Matter **20**, 365219 (2008).
[41] P. F. Schofield and S. A. T. Redfern, J. Phys.: Condens. Matter **4**, 375 (1992).
[42] M. Nicol and J. F. Durana, J. Chem. Phys. **54**, 1436 (1971).